

# Universality split in absorbing phase transition with conserved field on fractal lattices

Sang-Gui Lee and Sang B. Lee\*

*Department of Physics, Kyungpook National University, Daegu 702-701, Korea*

(Received 4 January 2008; published 23 April 2008)

The universality split in absorbing phase transition between the conserved lattice gas (CLG) model and the conserved threshold transfer process (CTTP) is investigated on a checkerboard fractal and on a Sierpinski gasket. The critical exponents  $\theta$ ,  $\beta$ ,  $\nu_{\parallel}$ , and  $z$ , which are associated with, respectively, the density of active particles in time, the order parameter, the temporal correlation length, and the dynamics of active particles, are elaborately measured for two models on selected fractal lattices. The exponents for the CLG model are found to be distinctly different from those of the CTTP model on a checkerboard fractal, whereas the two models exhibit the same critical behavior on a Sierpinski gasket, indicating that the universality split between the two models occurs only on a checkerboard fractal. Such a universality split is attributed from the dominant hopping mechanisms caused by the intrinsic properties of the underlying fractal lattice.

DOI: [10.1103/PhysRevE.77.041122](https://doi.org/10.1103/PhysRevE.77.041122)

PACS number(s): 05.70.Ln, 05.50.+q, 64.60.Ht

## I. INTRODUCTION

Nonequilibrium phase transition from a fluctuating phase into one or more absorbing states has attracted great interest for more than a decade [1–3]. Such an absorbing phase transition can be categorized to a finite number of universality classes. The most prominent and robust universality class is the directed percolation (DP) class. A wide variety of models with different evolution rules which satisfy the DP hypothesis [4,5] were found to belong to the DP class [6,7]. There are other known universality classes such as the parity conserving (PC) class [8–11] and the pair-contact process with diffusion class [12]; the critical behavior of the latter is still under debate mainly due to a slow convergence to the asymptotic limit [13–15]. The triplet and quadruplet reaction-diffusion models were also claimed to belong to the new universality class [16,17].

Recently, it was discovered that the absorbing phase transition with order parameters locally coupled to a nondiffusive conserved field generated a new universality class [18,20]. The stochastic sandpile model [21], the conserved threshold transfer process (CTTP) [22], and the conserved lattice gas (CLG) model were found to belong to this universality class [20]. The CLG model has a stochastic short-range interaction and exhibits a continuous transition from an active phase to an absorbing state at the critical density. In the CLG model, initially  $\rho N$  particles are distributed randomly on a lattice of  $N$  sites and each lattice site is either empty or occupied by one particle. A particle is defined to be active if it has at least one particle in the nearest-neighbor site and, otherwise, it is considered to be inactive. The dynamics proceed as that each active particle tends to hop to one of its nearest-neighbor empty sites, mimicking the repulsive interaction. In the CTTP model, on the other hand, each lattice site may be empty, occupied by one particle, or occupied by two particles. Empty and singly occupied sites are considered to be inactive, whereas doubly occupied sites are active. One tries to transfer both particles on a given active site to

randomly selected nearest-neighbor inactive sites. If all neighboring sites are occupied by two particles, the transfer stops. In both the CLG and the CTTP models, the density of active particles (or sites)  $\rho_a$  is the quantity which separates the active phase from the inactive phase. There is no particle creation or annihilation, and no self-diffusion; therefore, the number of particles is conserved during the process. This conservation law is known to produce a new universality class.

Lübeck and his collaborators carried out extensive simulations of the CLG model from two to five dimensions [23] and the CTTP model from one to six dimensions [24,25]. The critical exponents for the two models were found to be similar for the dimensionality  $d \geq 2$ , indicating that the CLG model and the CTTP model belong to the same universality class. However, in one dimension, the order parameter exponent and the exponents associated with the spatial and temporal correlation lengths were obtained, respectively, as  $\beta = 0.382$ ,  $\nu_{\perp} = 1.760$ , and  $\nu_{\parallel} = 2.452$  for the CTTP model [25], while the analytical work by de Oliveira and the numerical work by the present authors suggested  $\beta = \nu_{\perp} = 1$ , and  $\nu_{\parallel} = 4$  for the CLG model [26,27]. These results clearly indicate that the two models belong to different universality classes, i.e., the universality split occurs in one dimension.

This universality split has attracted attention only recently. The two features of the CLG model which are distinct from the CTTP model are proposed as possible causes of such universality split. One feature is the  $Z_2$  symmetry of the absorbing states at criticality, i.e., two symmetric absorbing states 010101... and 101010... exist at the critical density  $\rho_c = 0.5$  for the CLG model, whereas many absorbing states exist for the CTTP model. It should be noted that a single absorbing state with all sites singly occupied (i.e.,  $\rho_c = 1.0$ ) may be possible for the CTTP model; however, due to a noise, the critical density was known to be  $\rho_c = 0.969\ 29$  [24]. The other is the hopping mechanism of active particles. In the CLG model, the hopping of active particles is deterministic due to a dimensional reduction; since each active particle has an occupied nearest-neighbor site in one of the two directions and an empty site in an opposite direction, the site to which an active particle jumps is determined by a local conformation, rather than by random selection. In the CTTP

\*Corresponding author; [sblee@knu.ac.kr](mailto:sblee@knu.ac.kr)

model, on the other hand, since each active site may have one or two neighboring inactive sites which are either empty or singly occupied, the sites to transfer the particles may be determined stochastically. According to Lübeck and Heger, about 40% of the relaxation events are deterministic and the remaining 60% are stochastic in the one-dimensional CTTP model [25]. These features are typical only in one dimension, and it has been conjectured that one of these or both might be responsible for the universality split in one dimension.

In this paper, the critical behaviors of the CLG model and the CTTP on a checkerboard fractal (also known as the Vicsek fractal) and on a Sierpinski gasket are investigated, focusing on the universality split. This work was motivated from the recent work by Lee and Kim [28], which investigated the critical behavior of the CLG model on the same fractal lattices. It was found that the order parameter exponent of the CLG model on a checkerboard fractal lay between the one-dimensional (1D) value and the two-dimensional (2D) value of the CLG model, whereas on a Sierpinski gasket, it lay between the 1D and 2D values of the CTTP model. They conjectured that such a difference was attributed to the universality split on a checkerboard fractal, whereas no split was expected on a Sierpinski gasket. In this work, the critical exponents of the CTTP model on a checkerboard fractal and on a Sierpinski gasket are directly measured to clarify the possible universality split.

All critical exponents of the CTTP model on a checkerboard fractal are found to be different from those of the CLG model, whereas the critical exponents on a Sierpinski gasket are similar for both models, indicating that the universality split between the two models occurs only on a checkerboard fractal. Such a universality split is manifested by the dominant deterministic hopping mechanism on a checkerboard fractal.

The layout of this paper is as follows. In Sec. II, the models and the simulation methods are described. In Sec. III, the results for the CTTP model are presented and compared with those of the CLG model obtained by Lee and Kim [28] and also with the results obtained in this work for comparison. In Sec. IV, results are summarized and the concluding remarks are made to close the paper.

## II. MODELS AND SIMULATION METHODS

The generation of the checkerboard fractal and the Sierpinski gasket [29] is simple, and the details of the methods were described in Ref. [28]. The fractal dimension of the checkerboard fractal is  $d_F^{CB} = \ln 5 / \ln 3 \approx 1.465$  and that of the Sierpinski gasket is  $d_F^{SG} = \ln 3 / \ln 2 \approx 1.585$ .

For the simulation of the CTTP model, since initially particles are distributed randomly over the lattice, the dynamics of the particles near edges of the lattice might be different from the dynamics of the particles at the middle because the system is finite; therefore, the size of the system may affect the dynamics. This is a different situation from other models in which the defect (seed) simulation can be carried out from the center of the lattice; in such a case, the size of the system yields a null effect until the time when particles spread up to the edge of the system. In order to minimize the size effect,

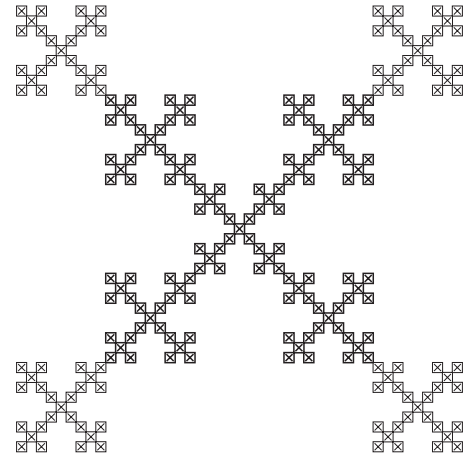


FIG. 1. A sample checkerboard fractal generated up to the third order (marked as thick squares), with parts of the periodically placed replicated cells at the four corners (marked as thin squares). The coordinate directions are set along the two diagonal directions, assuming that any two nearest-neighbor sites along the diagonal directions are connected.

the “periodic” boundary condition is set. For a checkerboard fractal, such a periodic boundary condition was previously employed by Lee and Kim [28]. Assuming that the current cell is the central subcell of a larger cell of one higher order, the replicated cells are assumed at the four corners. When particles exit the cell through the corner sites, the particles are assumed to reenter the cell through the sites at the opposite corners or, vice versa. The sample fractal lattice with parts of the periodically placed replicated cells is shown in Fig. 1.

For a Sierpinski gasket, on the other hand, the situation is different from that for the checkerboard fractal. (Note that Lee and Kim employed the “reflective” boundary condition for a Sierpinski gasket.) Assuming that the lattice generated is a subcell of the larger lattice of a higher-order generation, the three replicated cells may be assumed at the three corners, as shown in Fig. 2. When a particle exits through the site *B* or *C*, it can be assumed to reenter through the site *A* along the same direction as it exited because *A* is the site in

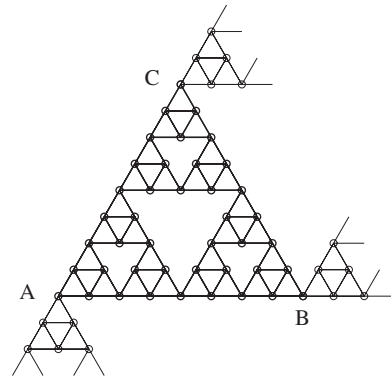


FIG. 2. A sample Sierpinski gasket generated up to the third order (marked as thick lines), with parts of the periodically placed three replicated cells (marked as thin lines). The lattice sites are assumed at the vertices of the triangles.

the main cell corresponding to the sites  $B$  and  $C$  in the replicated cells. When a particle exits through the site  $A$ , it should reenter the cell through  $C$  because the site  $C$  is the corresponding site of  $A$  in the lower-left replicated cell. However, if the particle exits through  $B$  and reenters through  $A$  and then the same particle exits through  $A$ , it should reenter the cell through  $B$  (rather than through  $C$ ). This is because, by periodicity, when a particle exits the cell through the site  $B$ , the particle stays in the right neighboring cell. When the same particle exits the cell through  $A$ , the particle in the right nearby cell goes back to the original cell through  $B$ . Therefore, those particles exiting through  $B$  and reentering the cell through  $A$  should be distinguished from other particles. Those particles are distinguished by coloring and, when a colored particle exits the cell through  $A$ , it is assumed to reenter the cell through  $B$ . This prescription allows the application of the periodic boundary condition for a Sierpinski gasket.

The simulation for the CTTP model is performed as follows. Initially,  $\rho N$  particles are distributed randomly in a given cell and each lattice site is allowed to be occupied by up to two particles. The doubly occupied sites, i.e., the active sites, are stored in the list. At each simulation step, an active site is randomly selected and both particles on the site attempt to transfer to the randomly chosen nearest-neighbor inactive sites, i.e., to the vacant or singly occupied sites. When no more inactive sites are available, the transfer stops. The evolution time is increased by  $1/N_a$ ,  $N_a$  being the number of active sites at time  $t$ .

For  $\rho > \rho_c$ , the density of active sites (or particles)  $\rho_a$  converges to the steady-state density  $\rho_{\text{sat}}$  as the evolution time increases. The steady-state density represents the ordering of the system; i.e., if  $\rho_{\text{sat}} > 0$ , the system is in the supercritical region and, if  $\rho_{\text{sat}} = 0$ , the system is in the subcritical region. At  $\rho_c$ ,  $\rho_a$  decreases in time algebraically as

$$\rho_a(t) \sim t^{-\theta}, \quad (1)$$

$\theta$  being the critical exponent. As  $\rho \rightarrow \rho_c$ , the order parameter decreases, following the power law

$$\rho_{\text{sat}}(\rho) \sim (\rho - \rho_c)^\beta, \quad (2)$$

and eventually becomes 0 at the critical density.

Most of the simulations on a checkerboard fractal are performed on the lattice of the seventh generation with 78 125 lattice sites, and those on a Sierpinski gasket on the lattice of the eleventh generation with 265 722 sites. However, whenever a larger system is determined as necessary, the lattices of up to eighth order and twelfth order are generated for the checkerboard fractal and the Sierpinski gasket, respectively.

### III. RESULTS AND DISCUSSIONS

#### A. On a checkerboard fractal

The CLG model on a checkerboard fractal was recently studied by Lee and Kim [28] and the critical exponents  $\theta$ ,  $\beta$ ,  $\nu_{\parallel}$ , and  $z$  were calculated from the power-law behaviors and the scaling analyses. In their work, particles with at least one occupied nearest-neighbor site were considered to be active.

In this rule, those particles which were trapped by being surrounded by other particles were considered to be active and they were counted in calculating the density of active particles. In the present work, on the other hand, only those particles which have at least one nearest-neighbor empty site to hop are considered to be active. For the sake of consistency, when the trapped particles are included in calculating the density of active particles, those particles should be selected with an equal probability to hop and the time should be elapsed even though they cannot move. From the universality concept, it is believed that such a detailed rule does not alter the critical behavior. Indeed, it was found that such a difference in the rule did not influence the critical behavior on a regular lattice in one and two dimensions (not shown). However, for a checkerboard fractal, such a rule does affect the critical behavior. In what follows, the results obtained by the latter rule are presented because the active site is assumed similarly for the CTTP model. The results are also compared with those of Lee and Kim, and the physical interpretation of the difference is provided.

In the usual absorbing phase transitions, the density of active particles decreases algebraically as in Eq. (1) at the critical density. However, for the models with a conserved field, it is not simple to determine  $\rho_c$  from the power-law behavior of  $\rho_a$  because of the finite size effect. For a density close to  $\rho_c$ , it was found that the density of active particles showed a power-law behavior for several decades and, afterwards, it decreased rapidly, as Rossi *et al.* observed for the CLG model on a square lattice [20] and also Lee and Kim observed for the CLG model on fractal lattices [28]. If, however,  $\rho_c$  was found from the power-law behavior of  $\rho_a$  in the long time limit, the value of  $\rho_c$  would have been overestimated and, with this value, the order parameter against the distance from the criticality would not have yielded the power-law behavior and both the off-critical scaling and the finite-size scaling would not have been satisfactory. Therefore, it is not satisfactory to determine  $\rho_c$  from the power-law behavior of  $\rho_a$  alone. In this work, the value of  $\rho_c$  which yields the best power-law behavior for the density of active particles in the region  $10 \leq t \leq 10^6$  is predetermined and, with this value, the power-law behavior of  $\rho_{\text{sat}}$  in Eq. (2), the off-critical scaling, and the finite-size scaling are analyzed. The initial particle density, which shows the best results for these tests, is determined as the critical density.

Plotted in Fig. 3 are the densities of active sites in time at the critical density of  $\rho_c = 0.8710$  for three different-size systems for the CTTP model, in comparison with the data for the CLG model at  $\rho_c = 0.6399$ . The exponent  $\theta$  may be obtained either from the regression fit of the data, as shown in the main plot, or from the analysis of local slope, defined by

$$\delta = - \frac{\ln[\rho_a(t)/\rho_a(t/m)]}{\ln m}, \quad (3)$$

plotted against the inverse time, as shown in the inset. Apparently  $\delta \rightarrow \theta$  as  $t \rightarrow \infty$ . In the inset, the upper plot is for the CLG model and the lower plot is for the CTTP model, both using  $m=10$ . A sharp increase in the  $t \gg 1$  region on both plots is reflected from the sharp decrease of  $\rho_a(t)$  in the main plot, due apparently to the finite-size effect. Neglecting such

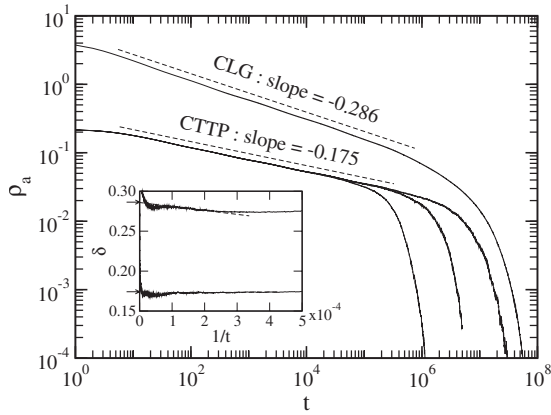


FIG. 3. The density of active particles  $\rho_a$  for the CTPP model on the checkerboard fractal plotted against the evolution time, in comparison with the data for the CLG model. The lower graphs are for the CTPP model at  $\rho_c=0.8710$  on lattices generated up to the sixth, seventh, and eighth generations and the upper data are for the CLG model at  $\rho_c=0.6399$ . The data for the CLG model are shifted upward by multiplying by 20 to avoid overlapping with the data for the CTPP model. The inset is the local slope plot for both models.

an anomaly, the intercepts on the ordinate are obtained as marked,  $\theta=0.175$  for the CTPP model and 0.286 for the CLG model, which are consistent with the regression fits in the main plot. The steady-state densities of active particles for the CTPP model are plotted in Fig. 4 against the distance from the criticality, in comparison with the data for the CLG model. From the figure,  $\beta=0.422$  is determined for the CTPP model. The values of  $\theta$  and  $\beta$  for the CTPP model are significantly smaller than the values of the CLG model,  $\theta=0.286$  and  $\beta=0.910$ . It is, thus, clear that the universality split between the CLG model and the CTPP model occurs on a checkerboard fractal. It should be noted that the estimates of  $\rho_c$  and  $\theta$  for the CLG model are consistent with those of Lee and Kim [28], while the estimate of  $\beta$  is significantly larger. The difference is attributed to the different rule used for determining active particles, as was described earlier in

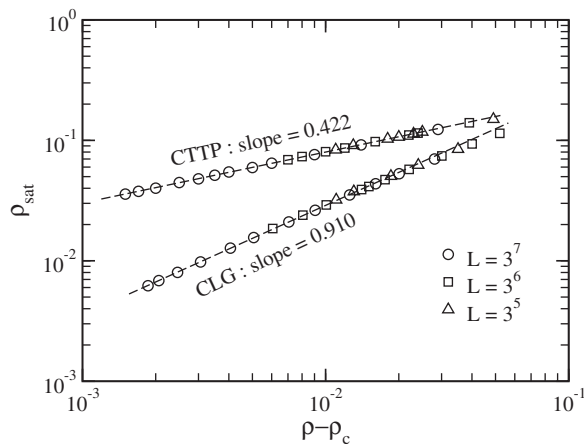


FIG. 4. The steady-state densities, i.e., the order parameters, of the CTPP model plotted on a double logarithmic scale against the distance from the criticality, in comparison with those of the CLG model.

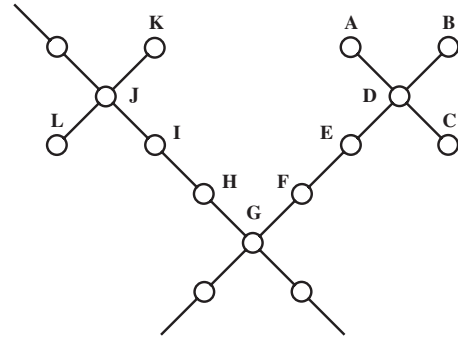


FIG. 5. Part of the lattice sites for the checkerboard fractal. The sites  $A, B, C, K,$  and  $L$  are the dead ends, and particles on the dead ends are trapped and cannot move.

this section. (Note that Lee and Kim obtained  $\theta=0.287$  and  $\beta=0.780$  [28].)

Intuitively, it is clear that the critical density remains the same no matter whether or not the trapped particles are considered to be active, because at  $\rho_c$  the system goes into an absorbing state, i.e., all particles are isolated and no trapped particles exist. However, the critical indices depend on the choice of the rules of determining active particles for the following reason. In practice, most trapped particles are those at dead ends such as the sites  $A, B, C, K,$  and  $L$  in Fig. 5. If the trapped particles at dead ends are considered to be active, those particles will be counted for the density of active particles even though they cannot move. If, on the other hand, they are considered to be inactive, those particles will not contribute to the dynamics except that they enable the particle at the nearby intersection site (such as the site  $D$ ) to become active. For this, however, a single dead end such as the site  $B$  plays the same role and the sites  $A$  and  $C$  are unnecessary. Therefore, any two of the three dead ends (sites  $A$  and  $C$ ) may be eliminated without altering the dynamics. Assuming that all such dead ends are eliminated, the dynamics of the CLG model on the new lattice remain unchanged. Therefore, the CLG model, when trapped particles are considered to be inactive, is practically the same as the CLG model on a lattice with effectively a smaller fractal dimension. Since the lattice dimensionality is known to be relevant in the usual critical behavior, the critical behavior of the CLG model on the lattice of smaller fractal dimension is expected to be different from the original checkerboard fractal. The critical indices on a lattice of smaller fractal dimension will, thus, become closer to the 1D values. The estimated value of  $\beta=0.910$  is indeed larger than that of Lee and Kim and is closer to the 1D value of  $\beta=1.0$ . Similarly, the exponent  $\nu_{||}$  is also found to be closer to the 1D value, as will be shown later.

The estimates of  $\beta$  and  $\theta$  may be verified by the off-critical scaling of the density of active particles,

$$\rho_a(t) = t^{-\theta} \mathcal{F}(t/\xi_{||}) = t^{-\theta} \mathcal{F}(t|\rho - \rho_c|^{\nu_{||}}). \quad (4)$$

Since, in the limit of  $t \rightarrow \infty$ ,  $\rho_a \rightarrow \rho_{\text{sat}} \propto (\rho - \rho_c)^\beta$  for  $\rho > \rho_c$ , it is expected that the scaling relation

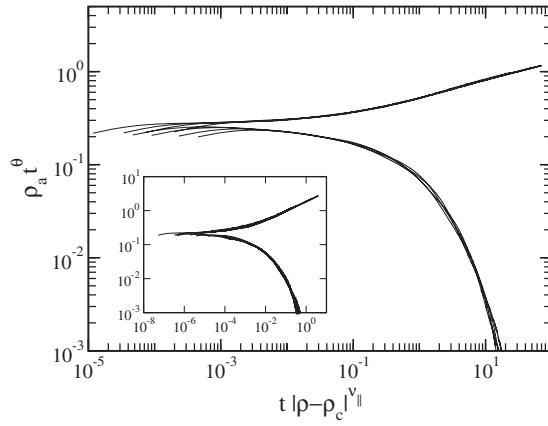


FIG. 6. The off-critical scaling function of the active particle densities for the CTTP model on a checkerboard fractal. Data are for  $\rho=0.83, 0.84, 0.85$ , and  $0.855$  (below) and for  $\rho=0.88, 0.885, 0.89$ , and  $0.90$  (above), using the estimates  $\theta=0.175$  and  $\nu_{\parallel}=2.41$ . The inset is the plot for the CLG model using  $\theta=0.286$  and  $\nu_{\parallel}=3.18$ .

$$\nu_{\parallel} = \beta/\theta \quad (5)$$

holds. This implies that, using the value of  $\nu_{\parallel}$  obtained from the scaling relation, the scaled data of  $\rho_a t^{\theta}$  plotted against the scaled variable  $x \equiv t|\rho - \rho_c|^{\nu_{\parallel}}$  should collapse onto the two universal curves, one for  $\rho > \rho_c$  and the other for  $\rho < \rho_c$ . The scaling function was analyzed with the data on a checkerboard fractal to verify the estimates of  $\theta$  and  $\beta$ .

Figure 6 shows the scaling function in Eq. (4) of the data for the CTTP model for selected values of  $\rho$  using the estimated values  $\theta=0.175$  and  $\nu_{\parallel} = \frac{0.422}{0.175} \approx 2.41$ . Data for different values of  $\rho$  collapse onto the two universal curves for  $\rho > \rho_c$  (above) and for  $\rho < \rho_c$  (below), implying that the estimates of  $\theta$  and  $\beta$ , and also the scaling relation are correct. For the CLG model, data also scale for  $\theta=0.286$  and  $\nu_{\parallel} = 0.91/0.286 \approx 3.18$ , as shown in the inset, indicating the estimates of this work for the CLG model are also correct. It should be noted that the looking poor collapsing for the data for  $\rho < \rho_c$  is due to an oscillatory or wiggling behavior of  $\rho_a(t)$  caused presumably by the underlying lattice geometry, as was observed previously [28]. The value of  $\nu_{\parallel}$  is also different from that of Lee and Kim obtained for the CLG model. The difference is apparently attributed to the different rule for determining active particles, as was discussed earlier.

The spatial correlation length characterized by  $\xi_{\perp} \sim |\rho - \rho_c|^{-\nu_{\perp}}$  are associated with the temporal correlation length via  $\xi_{\parallel} \sim |\rho - \rho_c|^{-\nu_{\parallel}} \sim \xi_{\perp}^z$ , where

$$z = \nu_{\parallel}/\nu_{\perp}. \quad (6)$$

The index  $z$  is also associated with the rms spreading distance via  $R \sim t^{1/z}$ . For a finite-size system, since the spatial correlation length cannot exceed the size of the system, i.e.,  $\xi_{\perp} \sim L$ , the scaling relation in Eq. (4) becomes, at  $\rho_c$ ,

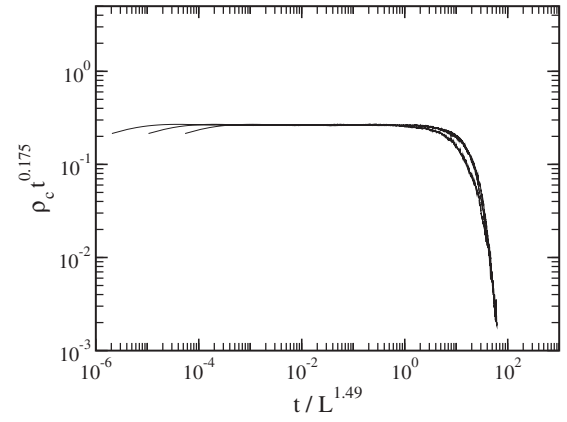


FIG. 7. The finite-size scaling function  $\rho_a t^{\theta}$  of the CTTP model on a checkerboard fractal plotted against the scaled time  $t/L^z$ . Data generated on lattices of the sixth, seventh, and eighth generations exhibited the best collapsing for  $\theta=0.175$  and  $z=1.49$ .

$$\rho_a(t) = t^{-\theta} \mathcal{G}(t/L^z). \quad (7)$$

Thus, the scaled density of active particles for various size systems fall on the same curve when plotted against the scaled time, yielding the finite-size scaling. Plotted in Fig. 7 are the scaled density  $\rho_a t^{\theta}$  against the scaled time  $t/L^z$ . The scaled data of Fig. 3 for  $L=3^6, 3^7$ , and  $3^8$ , obtained using the adjustable parameter  $z=1.49$  indeed collapse onto the same curve. Here the data for systems of only the three largest sizes were plotted because it was not possible to set up the critical density for systems that are too small. For example, for  $L=3^4$ , the number of particles to be distributed at criticality is 544.4; if 545 particles are distributed, the density will exceed the critical density. Since each additional particle affects much on the density, we found that it was hard to expect the data collapsing for the too small systems. (Note that the deviation at the veer-down region is due to the different decaying behavior at the large  $t$  region in Fig. 3.) It should be emphasized that, for the CLG model, the finite-size scaling plot as in Eq. (7) cannot not be provided. Failure of the scaling is caused by the different asymptotic behaviors at  $\rho_c$  between the smaller systems and the larger systems. For the smaller systems the density of active particles saturated even at  $\rho_c$  and for the larger systems it decayed. This kind of behavior for the CLG model is again different from that of the CTTP model, indicating that the two models exhibit different behaviors.

If the exponent  $\nu_{\perp}$  associated with the spatial correlation length is calculated from the scaling relation in Eq. (6),  $\nu_{\perp} = 2.41/1.49 = 1.62$  would be obtained. However, it was found previously that, in one dimension, Eq. (6) was not satisfied with the known results [27]. A similar violation of the scaling relation was first observed by Dickman *et al.* in one dimension [30] and by others in higher dimensions [18–20], where the scaling relation in Eq. (5) was claimed to be violated by an anomaly of the exponent  $\theta$ . In one dimension, since the dynamics of the CLG model becomes deterministic due to the reduction of the dimensionality, the critical exponents may be calculated exactly. Indeed, de Oliveira calculated analytically the exponents  $\beta$  and  $\nu_{\perp}$  [26]. By numerical

simulation,  $\nu_{\parallel}$ ,  $z$ , and  $\nu_{\perp}$  were calculated by the present authors [27] and the scaling relation in Eq. (5) was found to be satisfied but the relation in Eq. (6) was not. Therefore, for the CLG model on a checkerboard fractal, since information on the validity of the scaling relations is unknown, the value of  $\nu_{\perp}$  is not determined in this work.

The critical exponent  $\nu_{\perp}$  can be estimated from the finite-size scaling of the steady-state density at criticality, which may be written as a function of the size of the system and the spatial correlation length, but not a function of two variables but of the ratio of two, i.e.,

$$\rho_{\text{sat}}(\rho, L) = |\rho - \rho_c|^{\beta} h(L|\rho - \rho_c|^{\nu_{\perp}}) = L^{-\beta/\nu_{\perp}} \mathcal{H}(L|\rho - \rho_c|^{\nu_{\perp}}). \quad (8)$$

At  $\rho = \rho_c$ , the steady-state density should scale as  $\rho_{\text{sat}} \sim L^{-\beta/\nu_{\perp}}$ . In this scaling,  $\rho_{\text{sat}}$  should be calculated from those samples which survive and exhibit the steady-state densities. The surviving samples are those samples which survive up to  $t$  time steps. Suppose that sampling up to  $t_{\text{max}}$  steps is intended. Then, the samples survived up to  $t (< t_{\text{max}})$  steps and fallen into an absorbing state afterward are included in the average up to  $t$  steps. The number of samples, thus, decreases as  $t$  increases. With this average, it was found that the density of active particles decreased slowly as  $t$  increased up to  $10^8$  steps and, accordingly, it was not possible to estimate  $\rho_{\text{sat}}$  in the  $t \rightarrow \infty$  limit (not shown). However, it was found that this is particular only on a fractal lattice. For a regular square lattice, both the CLG and CTPP models were found to yield steady-state density and  $\rho_{\text{sat}}$  displayed correct power-law behavior when plotted against the size of system. If, on the other hand, it is assumed that the survived samples are those which survived all the way up to  $t_{\text{max}}$  steps,  $\rho_{\text{sat}}$  will depend on the choice of  $t_{\text{max}}$ . It was found that, right at  $\rho_c$ , the system was in a close vicinity to the absorbing state and it went into an absorbing state at a certain moment. Therefore, if  $t_{\text{max}}$  is set large, the very rare samples will survive and the steady-state density will depend upon the choice of  $t_{\text{max}}$ . Therefore, for the CLG model on a checkerboard fractal, it was not possible to estimate  $\nu_{\perp}$  from the scaling of  $\rho_{\text{sat}}$  at the criticality.

**B. On a Sierpinski gasket**

In Fig. 8, the densities of active sites for the CTPP model for selected sizes of systems are plotted, i.e., for  $L=2^8, 2^9, 2^{10}$ , and  $2^{11}$  at  $\rho=0.7763$  at which the best linear behavior is observed until the time before the data veered down, in comparison with the data for the CLG model at  $\rho_c=0.31790$ . (Note that the data by Lee and Kim for the CLG model was used and the plot is shifted upward to avoid overlapping.) The regression slopes of the plots are  $\theta=0.242$  for the CTPP model and 0.244 for the CLG model. These two values are consistent within the errors, implying that the two models display the same critical behavior. The steady-state density is also calculated for the selected values of  $\rho$  in the supercritical region, and the results are shown in Fig. 9, in comparison with the data for the CLG model. Data for the two models for  $L=2^9, 2^{10}$ , and  $2^{11}$  show the slope similar to each other, i.e.,  $\beta=0.544$  for the CTPP model and  $\beta=0.547$  for the CLG

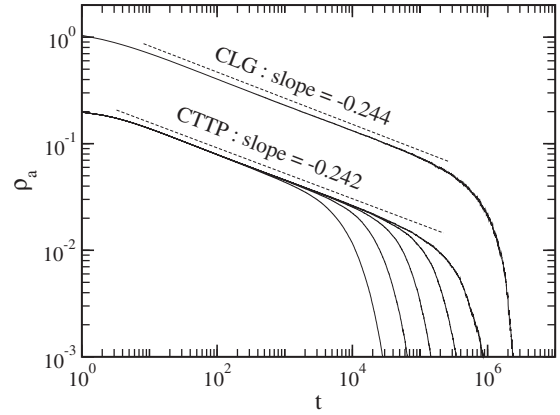


FIG. 8. The density of active sites  $\rho_a$  for the CTPP model on the Sierpinski gasket plotted against the evolution time, in comparison with the data for the CLG model. The lower graphs are for the CTPP model at  $\rho_c=0.7763$  on lattices of the seventh, eighth, ninth, tenth, and eleventh generations, and the upper data are for the CLG model at  $\rho_c=0.3179$ . The data for the CLG model are shifted upward by multiplying by 5 to avoid overlapping with the data for the CTPP model.

model, indicating that the two models yield the same value. (Note that the data in the small  $\rho - \rho_c$  region was focused on.) It should be noted that the exponent for the order parameter on a Sierpinski gasket lies between the 1D and the 2D values.

Simulations were also carried out as tests considering the trapped particles as being active and the results were consistent with those in Figs. 8 and 9. Since there is no dead end on a Sierpinski gasket, it is expected that the different rules of determining the active particles do not influence the critical behavior. The results support this hypothesis.

The off-critical scaling analysis and the finite-size scaling analysis are also carried out to verify the estimates  $\theta$  and  $\beta$ . Data plotted in Fig. 10 is the off-critical scaling function obtained using the value  $\nu_{\parallel}=2.25$  calculated from the scaling relation using the estimates of  $\beta$  and  $\theta$ . Data for various values of  $\rho > \rho_c$  fall on the same upper curve and those for  $\rho < \rho_c$  collapse onto the lower curve, displaying that the off-

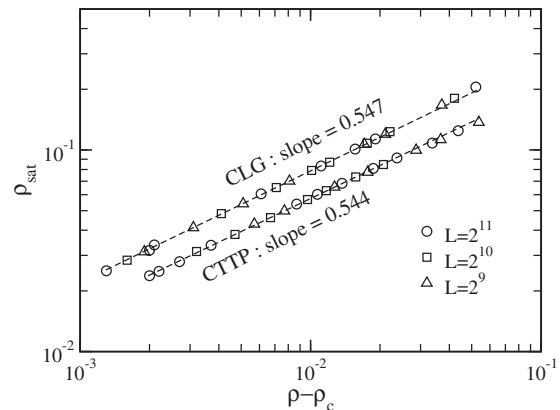


FIG. 9. The steady-state densities of active sites for the CTPP model plotted on a double logarithmic scale against the distance from the criticality, in comparison with those of the CLG model.

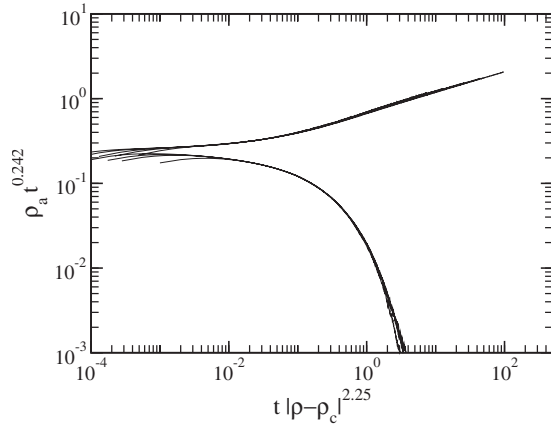


FIG. 10. The off-critical scaling function of the density of active sites against the scaled variable  $t|\rho - \rho_c|^{2.25}$  for  $\rho=0.73, 0.75, 0.755,$  and  $0.76$  (below) and for  $\rho=0.787, 0.79, 0.795, 0.80,$  and  $0.81$  (above), using  $\theta=0.242$  and  $\nu_{\parallel}=2.25$  for the CTTP model on a Sierpinski gasket.

critical scaling holds. Similar scaling was also observed previously for the CLG model. Considering the estimates of  $\theta$ ,  $\beta$ , and  $\nu_{\parallel}$ , it is concluded that the CTTP model on a Sierpinski gasket exhibits the critical behavior similar to the CLG model, implying that the two models belong to the same universality class.

The dynamic exponent  $z$  can be calculated from the finite-size scaling of  $\rho_a$  at the criticality, assuming that  $z$  is an adjustable parameter to the best data collapsing. The scaling function in Eq. (7) for the data on systems of  $L=2^8, 2^9, 2^{10},$  and  $2^{11}$  is plotted and the best collapsing is observed for  $z=1.30$ , as shown in Fig. 11. Thus, the dynamic exponent  $z=1.30$  is estimated for the CTTP model on a Sierpinski gasket. It should be noted that the value of  $z$  is smaller than that observed for the CLG model [28], where  $z=1.69$  was observed. (Note that the reflective boundaries were employed in the simulations of Lee and Kim for the CLG model, whereas the periodic boundaries were employed in this work

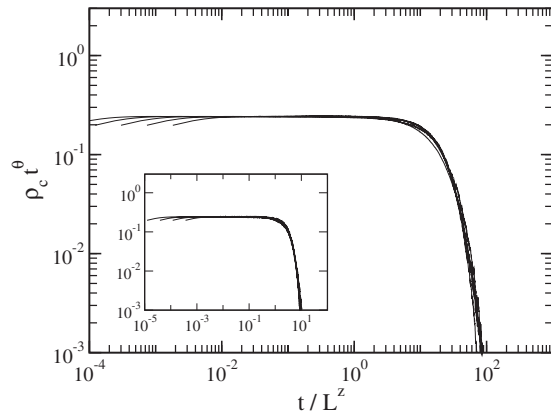


FIG. 11. The finite-size scaling function of the densities of active sites  $\rho_a t^{\theta}$  as a function of the scaled time  $t/L^z$  for the CTTP model on a Sierpinski gasket of the eighth, ninth, tenth, and eleventh generations. The main plot is the data for  $\theta=0.242$  and  $z=1.30$  using the periodic boundaries and the inset is those for  $\theta=0.242$  and  $z=1.63$  using the reflective boundaries.

TABLE I. The critical exponents of the CTTP and CLG models on fractal lattices, in comparison with those on a regular lattice in one and two dimensions.

	$\theta$	$\beta$	$\nu_{\parallel}$	$z$
1D:				
CTTP model <sup>a</sup>	0.141	0.382	2.452	1.393
CLG model <sup>b</sup>	0.25	1.0	4.0	2.0
Checkerboard:				
CTTP model	0.175	0.422	2.41	1.49
CLG model	0.286	0.910	3.18	
Sierpinski gasket:				
CTTP model	0.242	0.544	2.25	1.30
CLG model	0.244	0.547	2.24	1.69 <sup>c</sup>
2D:				
CTTP model	0.43(1) <sup>c</sup>	0.639 <sup>d</sup>		1.55(5) <sup>e</sup>
CLG model	0.43(1) <sup>c</sup>	0.63(1) <sup>e</sup>	1.225 <sup>a</sup>	1.52(6) <sup>e</sup>

<sup>a</sup>Reference [25].

<sup>b</sup>Reference [27].

<sup>c</sup>Results obtained using the reflective boundaries.

<sup>d</sup>Reference [24].

<sup>e</sup>Reference [20].

for the CTTP model.) In order to clarify the discrepancy of the dynamic exponent, simulations are carried out for the CTTP model on a Sierpinski gasket, using the reflective boundary condition. Data for various size systems are found to display a good collapsing for  $z=1.63$ , as shown in the inset of Fig. 11, which is much closer to the value that Lee and Kim obtained using the reflective boundaries.

The different values of  $z$  which yielded the data collapsing for the density of active particles were apparently attributed to the finite-size effect. As the size of the system increases, the influence of the boundary condition is expected to diminish and, for sufficiently large systems, the boundary condition should yield a null effect. Considering that the values of  $\theta$  and  $\beta$  were similar and the off-critical scaling held with the same value of  $\nu_{\parallel}$  for the CLG model and the CTTP model even though different boundary conditions were employed, it appeared that the exponents  $\theta$ ,  $\beta$ , and  $\nu_{\parallel}$  were not influenced by the boundary conditions, as expected from the universality concept. However, the exponent  $z$  which yielded the best data collapsing for the finite-size scaling varied depending on the boundary conditions employed. Therefore, the scaling relation in Eq. (6) is less reliable than the relation in Eq. (5) for absorbing phase transitions with a conserved field. This assertion agrees with the earlier observation in one dimension, in that the scaling relation in Eq. (6) was found to be violated for the exact exponents [27]. The source of such an anomaly was conjectured to be attributed to the finite-size effect.

Table I summarizes the estimates of the critical exponents for the CTTP and CLG models on a checkerboard fractal and on a Sierpinski gasket, in comparison with those on a regular lattice in one and two dimensions.

#### IV. SUMMARY AND CONCLUDING REMARKS

The critical behaviors of the CLG model and the CTTP model have been investigated on a checkerboard fractal and on a Sierpinski gasket. The checkerboard fractal has one, two, or four nearest-neighbor sites depending on the sites, while the Sierpinski gasket has a coordination number four. The critical exponents  $\theta$ ,  $\beta$ ,  $\nu_{\parallel}$ , and  $z$  were calculated for both models. The trapped particles which were surrounded by other particles were considered to be inactive because those particles could not move. The results for the CLG model were considerably different from those of Lee and Kim, for which particles with at least one occupied nearest-neighbor site were considered to be active no matter whether or not they were trapped. The physical interpretation of such different behaviors were provided.

On a checkerboard fractal, the critical exponents of the CLG model were considerably different from those of the CTTP. Considering that the two models on a regular lattice of the dimensionality  $d \geq 2$  are known to belong to the same universality class, it is clear that the universality split for the two models occurs on a checkerboard fractal. On a Sierpinski gasket, on the other hand, the two models exhibited the same critical exponents, indicating that both the CLG model and the CTTP model belong to the same universality class. A similar universality split was reported in one dimension, in which the two symmetric absorbing states exist and the hopping of the active particles was deterministic for the CLG model, whereas infinitely many absorbing states existed and the hopping was stochastic for the CTTP model. Therefore, it was possible to theorize that either the  $Z_2$  symmetry or the deterministic hopping (or both) for the CLG model might be responsible for such a universality split. On a checkerboard fractal, however, neither the  $Z_2$  symmetry existed nor the hopping was fully deterministic for the CLG model; nevertheless, the similar universality split occurred. It is, therefore, believed that the “dominant” deterministic hopping mechanism on a checkerboard fractal yielded the universality split.

Exactly 40% of the lattice sites on a checkerboard fractal are the dead ends, another 40% of the sites have two nearest-neighbor sites, and the remaining 20% have four nearest-neighbor sites. Since those particles on the dead ends cannot move and those on the sites with two nearest neighbors hop deterministically, more than 60% of the hopping is deterministic for the CLG model, whereas all jumps are stochastic unless all but one nearest-neighbor sites are active sites for the CTTP model. For a Sierpinski gasket, on the other hand,

since all sites have four nearest neighbors, all jumps are stochastic for both the CLG model and the CTTP model unless three neighboring sites are active. Therefore, it is clear that such a different hopping mechanism is the major source of the universality split.

One might suspect that any small amount of stochastic hopping may lead the system to flow toward the stable fixed point corresponding to the CTTP model. If then, it would be expected that the critical behavior of the CLG model crosses over to the CTTP behavior in the limits of  $L \rightarrow \infty$  and  $t \rightarrow \infty$ . Such a possible crossover is currently under investigation, designing a lattice model on a  $d$ -dimensional hypercubic lattice. In this new model, each site may be occupied by up to  $2d$  particles and the sites with  $2d$  particles are considered to be active. For each active site, one tries to transfer each particle to each nearest-neighbor site. This model is identical to the Bak-Tang-Wissenfeld (BTW) [31] finite-energy sandpile model [18,32], except that the number of particles to be occupied on each site is limited. The preliminary results indicated that  $\rho_{\text{sat}}$  was discontinuous at criticality and  $\rho_a(t)$  exhibited anomalous behavior, which appeared to yield the usual scaling analysis to fail. Such anomalies might be similar to those of the BTW model, where the simple scaling fails and the multifractal scaling might be useful [33]. In order to observe the influence of the stochastic hopping on the critical behavior, a small fraction of active sites are allowed to transfer particles stochastically. It was found that any small amount of stochasticity eliminated the anomalies and the usual scaling analysis appeared to work. In addition, increasing the amount of stochasticity, it was found that  $\rho_a(t)$  exhibited two power-law regions in time, which might be the precursor of a crossover from fully deterministic limit to stochastic CTTP limit. Moreover, when 20% of stochasticity was included in the dynamics, the system exhibited fully the CTTP critical behavior. In the present data for the CLG model on a checkerboard fractal, any precursor of a crossover was not observable and the stochasticity is no less than 20%; therefore, the system less likely crosses over to the CTTP fixed point and the universality split is believed to be a genuine behavior which is specific on a checkerboard fractal.

#### ACKNOWLEDGMENTS

This work was supported by the Korea Science and Engineering Foundation Grant No. R01-2004-000-10148-0 and the BK-21 project from the Ministry of Education, Korea Government.

[1] J. Marro and R. Dickman, *Nonequilibrium Phase Transitions in Lattice Models* (Cambridge University Press, Cambridge, UK, 1999).  
 [2] H. Hinrichsen, *Adv. Phys.* **49**, 815 (2000).  
 [3] G. Ódor, *Rev. Mod. Phys.* **76**, 663 (2004).  
 [4] H. K. Janssen, *Z. Phys. B* **42**, 151 (1981).  
 [5] P. Grassberger, *Z. Phys. B: Condens. Matter* **47**, 365 (1982).

[6] I. Jensen and R. Dickman, *Phys. Rev. E* **48**, 1710 (1993).  
 [7] M. A. Munoz, G. Grinstein, R. Dickman, and R. Livi, *Phys. Rev. Lett.* **76**, 451 (1996).  
 [8] I. Jensen, *Phys. Rev. E* **50**, 3623 (1994).  
 [9] H. Takayasu and A. Y. Tretyakov, *Phys. Rev. Lett.* **68**, 3060 (1992).  
 [10] S. Kwon and H. Park, *Phys. Rev. E* **52**, 5955 (1995).



- [11] J. Cardy and U. C. Täuber, Phys. Rev. Lett. **77**, 4780 (1996).
- [12] For the bosonic version, see M. J. Howard and U. C. Täuber, J. Phys. A **30**, 7721 (1997); for the fermionic version, see E. Carlon, M. Henkel, and U. Schollwöck, Phys. Rev. E **63**, 036101 (2001).
- [13] J. Kockelkoren and H. Chaté, Phys. Rev. Lett. **90**, 125701 (2003).
- [14] J. D. Noh and H. Park, Phys. Rev. E **69**, 016122 (2004).
- [15] H. Hinrichsen, Physica A **361**, 457 (2006).
- [16] K. Park, H. Hinrichsen, and I.-M. Kim, Phys. Rev. E **66**, 025101(R) (2002).
- [17] G. Ódor, Phys. Rev. E **67**, 056114 (2003).
- [18] A. Vespignani, R. Dickman, M. A. Muñoz, and S. Zapperi, Phys. Rev. Lett. **81**, 5676 (1998); Phys. Rev. E **62**, 4564 (2000).
- [19] R. Dickman, M. A. Muñoz, A. Vespignani, and S. Zapperi, Braz. J. Phys. **30**, 27 (2000).
- [20] M. Rossi, R. Pastor-Satorras, and A. Vespignani, Phys. Rev. Lett. **85**, 1803 (2000).
- [21] S. S. Manna, J. Phys. A **24**, L363 (1991).
- [22] J. F. F. Mendes, R. Dickman, M. Henkel, and M. C. Marques, J. Phys. A **27**, 3019 (1994).
- [23] S. Lübeck, Phys. Rev. E **64**, 016123 (2001).
- [24] S. Lübeck, Phys. Rev. E **66**, 046114 (2002).
- [25] S. Lübeck and P. C. Heger, Phys. Rev. E **68**, 056102 (2003).
- [26] M. J. de Oliveira, Phys. Rev. E **71**, 016112 (2005).
- [27] S. G. Lee and S. B. Lee, Phys. Rev. E **77**, 021113 (2008).
- [28] S. B. Lee and Y. N. Kim, Phys. Rev. E **76**, 031137 (2007).
- [29] T. Vicšek, *Fractal Growth Phenomena* (World Scientific, Singapore, 1992).
- [30] R. Dickman, M. Alava, M. A. Muñoz, J. Peltola, A. Vespignani, and S. Zapperi, Phys. Rev. E **64**, 056104 (2001).
- [31] P. Bak, C. Tang, and K. Wiesenfeld, Phys. Rev. Lett. **59**, 381 (1987); Phys. Rev. A **38**, 364 (1988).
- [32] R. Dickman, A. Vespignani, and S. Zapperi, Phys. Rev. E **57**, 5095 (1998).
- [33] M. DeMenech, A. L. Stella, and C. Tebaldi, Phys. Rev. E **58**, R2677 (1998); see also C. Tebaldi, M. De Menech, and A. L. Stella, Phys. Rev. Lett. **83**, 3952 (1999).